

Electronic Supplementary Material

Hyperbranched magnetic polymer: highly efficient removal of Cr(VI) and application in electroplating wastewater

Nan Sun, Qing Wu, Lifang Jin, Zichen Zhu, Jianhui Sun (✉), Shuying Dong, Haijiao Xie, Chunyan Zhang,
Yanrui Cui

Key Laboratory for Yellow River and Huai River Water Environmental and Pollution Control, Ministry of Education,
and Henan Key Laboratory for Environmental Pollution Control, School of Environment, Henan Normal University,
Xinxiang 453007, China

E-mail: sunjhhj@163.com

List of the Supplemental Texts

Text S1. Preparation of 2,4,6-Trihydrazino-1,3,5-triazine.

Text S2. Synthesis of Fe₃O₄ nanoparticles.

Text S3. The results of N₂ adsorption-desorption.

Text S4. Isotherm models.

Text S5. Kinetics models.

Text S6. Thermodynamic models.

List of the Supplemental Figures

Figure S1. (a) TT chemical synthesis diagram, (b) M-TT preparation process.

Figure S2. (a) SEM image of Fe₃O₄, (b) SEM image of M-TT. (c) TEM image of M-TT.

Figure S3. Comparison of M-TT magnetic separation before (a) and after (b).

Figure S4. (a) Distribution of pore diameter; (b) BET analysis of TT and M-TT.

Figure S5. XRD pattern of raw materials and products.

Figure S6. C1s(a), N1s(b), S2p(c), O1s(d), Fe2p(e)'s XPS high-resolution spectrum.

Figure S7. The Langmuir model and Freundlich isotherm model fitting of Cr(VI) adsorption onto M-TT (pH = 4.4, T = 298 K) (a), onto M-TT (pH = 4.4, T = 308 K) (b) and onto M-TT (pH = 4.4, T = 318 K) (c), and General drawing (pH = 4.4, T = 298 K, T=308 K, T=318 K) (d).

Figure S8. The fitting of the pseudo-first-order kinetic model (a), the pseudo-second-order (b) and

31 the intra-particle kinetic models (c, d) for Cr(VI) adsorption onto M-TT (pH = 4.4, T = 298 K, C₀ =
32 20 mg·L⁻¹).

33 **Figure S9.** Thermodynamic curve of Cr(VI) adsorption onto M-TT (pH = 4.4, T = 298 K, C₀ = 20
34 mg·L⁻¹).

35 **Figure S10.** Removal of Cr(VI) (a) and Cr (III) (b) by TT and M-TT (pH = 4.4, T = 298 K, C₀ = 20
36 mg·L⁻¹).

37

38

39 **List of the Supplemental Tables**

40 **Table S1.** N₂ adsorption-desorption parameters of the TT and M-TT composite.

41 **Table S2.** Two isotherm parameters for Cr(VI) adsorption onto M-TT (pH = 4.4, T = 298 K).

42 **Table S3.** Kinetic parameters for Cr(VI) adsorption onto M-TT (pH = 4.4, T = 298 K, C₀ = 20 mg·L⁻¹).
43

44 **Table S4.** Thermodynamic parameters for Cr(VI) adsorption onto M-TT at different temperatures.

45 The calculated adsorption energies of Cr atom on four sites of substrate material.

46 **Table S6.** Comparison before and after adsorption of other components in electroplating wastewater.

47

48

49 **Text S1**

50 A certain amount of absolute ethanol, cyanuric chloride and 80% hydrazine hydrate were added

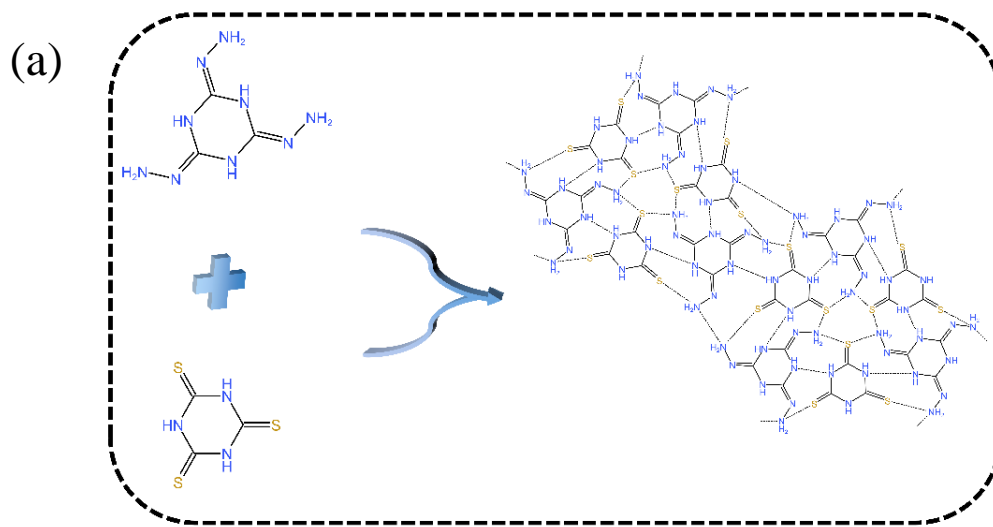
51 to a 250 ml three-necked flask, placed in a constant temperature oil bath heating stirrer, heated to 50 °C

52 and kept for 2 h. After that, Na₂CO₃ solution was added to the obtained liquid for washing with suction,

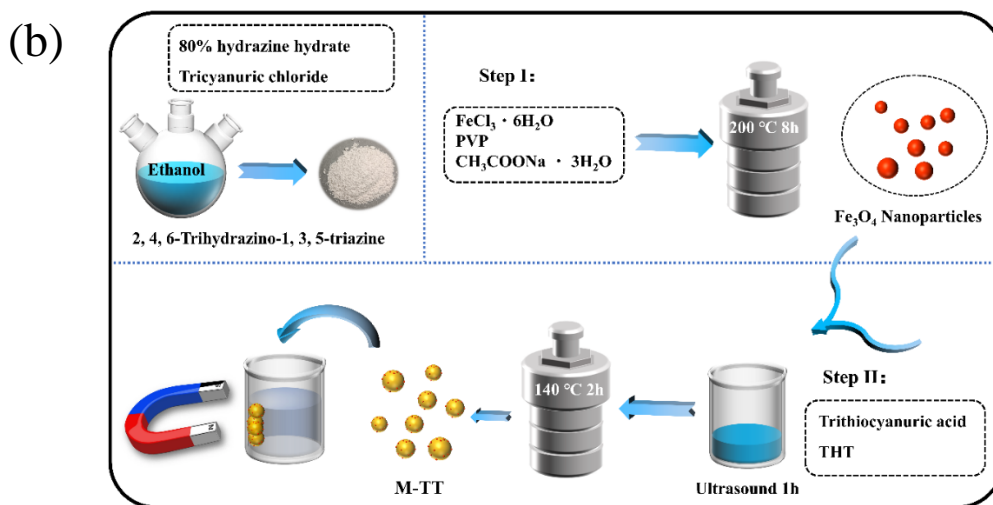
53 and the obtained product was dried in an oven at 85 °C for 12 h.

54

55 **Figure S1**



56



57

58

59

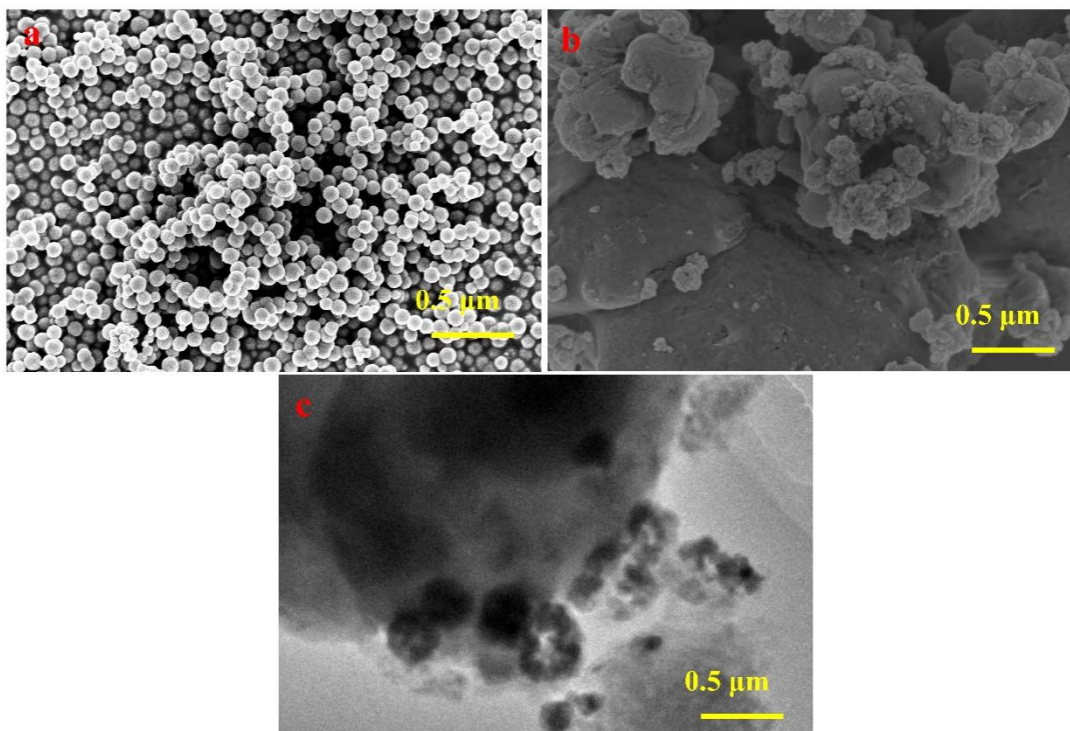
Fig. S1 (a) TT chemical synthesis diagram, (b) M-TT preparation process.

60 **Text S2**

61 Fe_3O_4 nanoparticles were prepared by solvothermal reduction method. Under vigorous stirring,
 62 3 g $\text{FeCl}_3 \cdot 6\text{H}_2\text{O}$, 4 g $\text{CH}_3\text{COONa} \cdot 3\text{H}_2\text{O}$ and 2 g polyvinylpyrrolidone (PVP) were dissolved in 60 mL
 63 of ethylene glycol. Then, the homogeneous mixture was transferred to a 100 mL stainless steel
 64 autoclave lined with Teflon, heated to 200 °C and held for 8 h. After that, a black precipitate was
 65 obtained by magnetic separation, washed with deionized water and ethanol, and dried in a vacuum
 66 oven at 60 °C for 12 h.

67

68 **Figure S2**



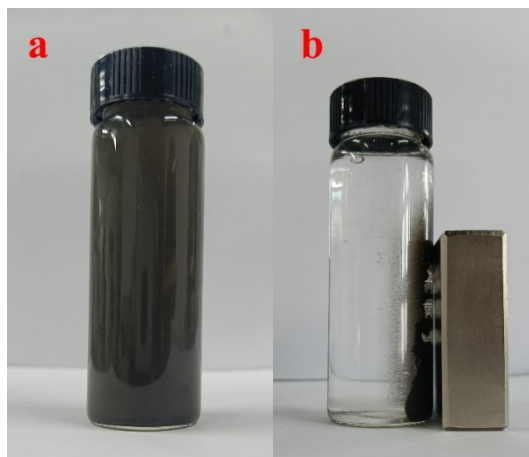
69

70

Fig. S2 (a) SEM image of Fe₃O₄, (b) SEM image of M-TT. (c) TEM image of M-TT.

71

72 **Figure S3**



73

74

Fig. S3 Comparison of M-TT magnetic separation before (a) and after (b).

75

76 **Text S3**

77

The specific surface area of M-TT determined by the BET method was about 28.9648 m²·g⁻¹

78

(Fig. S4a), and the specific surface area of TT was 39.4639 m²·g⁻¹. The pore sizes of both M-TT and

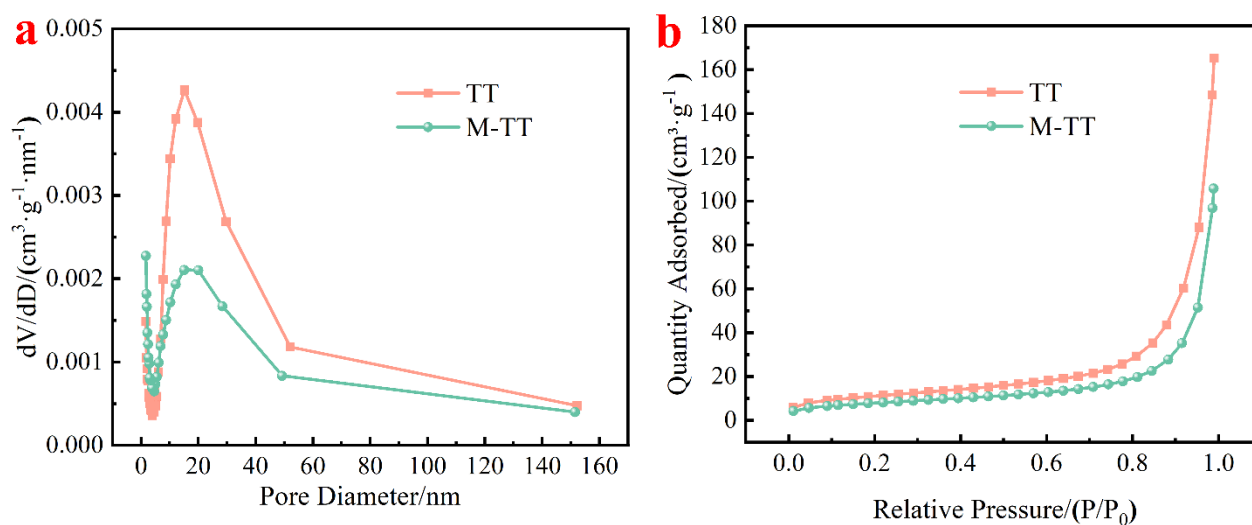
79

TT calculated by BJH analysis were in the range of 3-50 nm (Fig. S4b), indicating the presence of

80 mesopores in the prepared samples. There is clear absorption at higher relative pressures, indicating
81 the existence of mesopores in the material framework. The surface of M-TT material contains very
82 rich adsorption active sites, and the larger pore size can provide more ions with the opportunity to
83 contact the active sites, which is beneficial to enhance its adsorption performance.

84

85 **Figure S4**

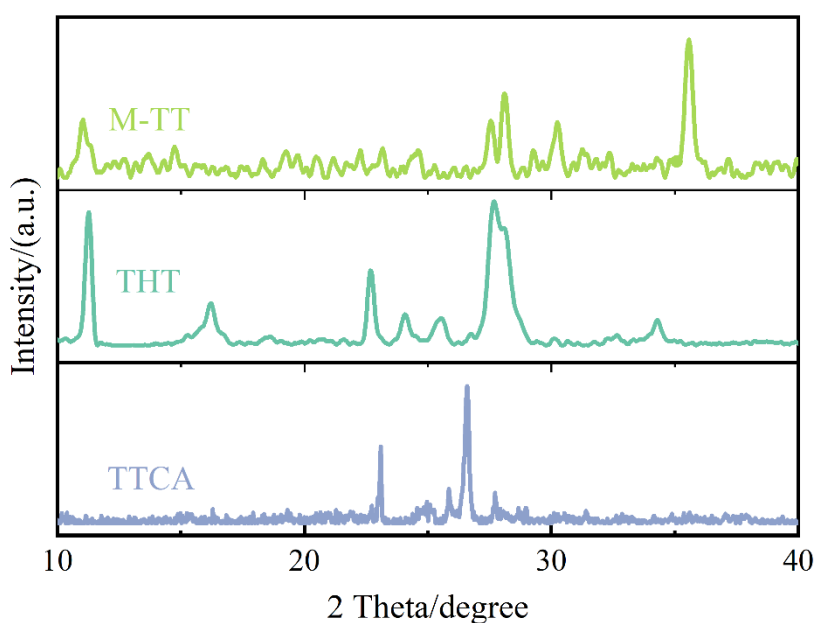


86

87

Fig. S4 (a) Distribution of pore diameter; (b) BET analysis of TT and M-TT.

88 **Figure S5**



89

90

Fig. S5 XRD pattern of raw materials and products.

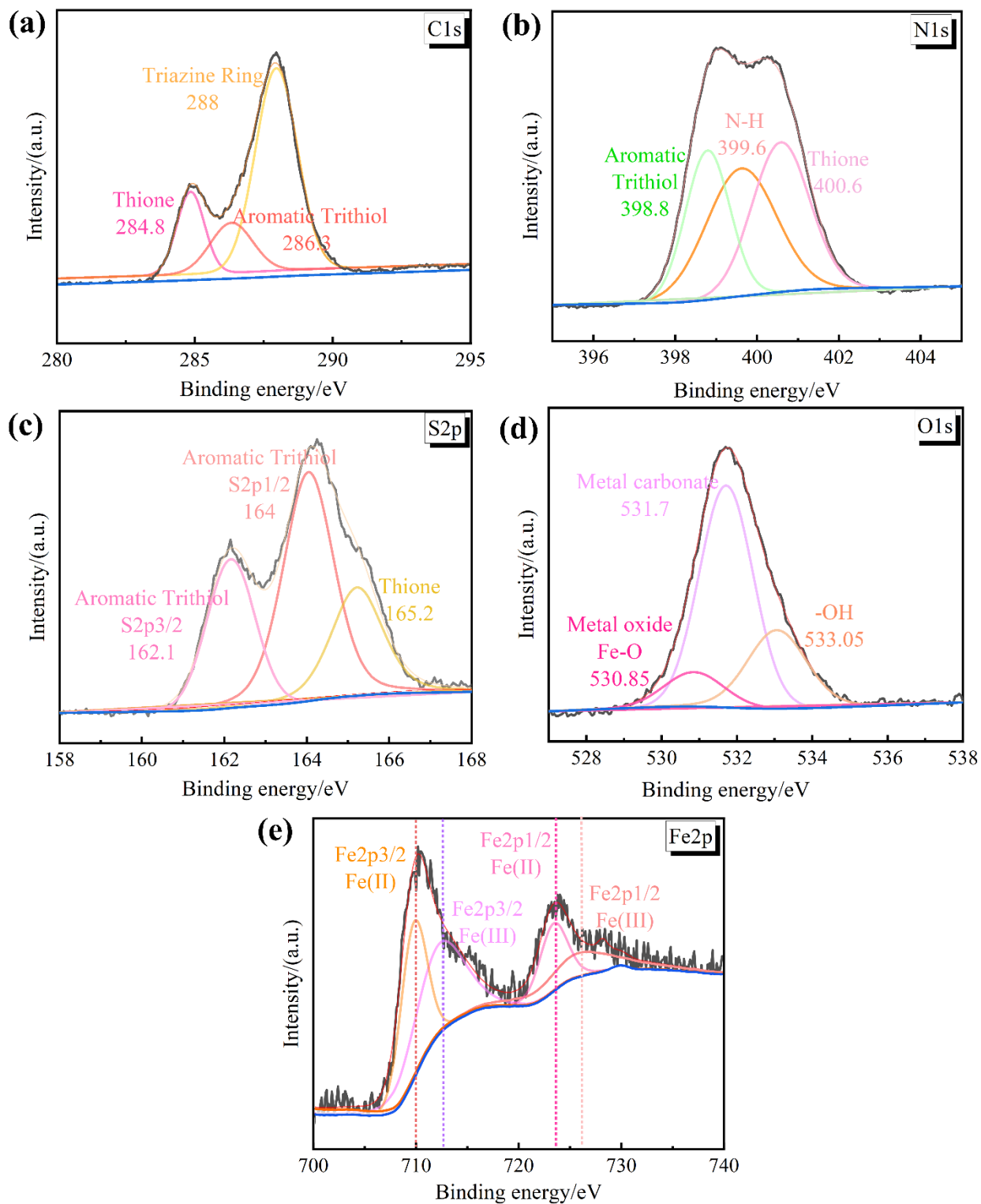


Fig. S6. C1s(a), N1s(b), S2p(c), O1s(d), Fe2p(e)'s XPS high-resolution spectrum.

92

93

94

95

96 **Text S4**

97

The Langmuir and Freundlich, separation factor (R_L) isotherm model is expressed as the equation

98 Eq. (1), Eq. (2), Eq. (3):

99
$$\frac{c_e}{q_e} = \frac{c_e}{q_m} + \frac{1}{q_m K_L} \quad (1)$$

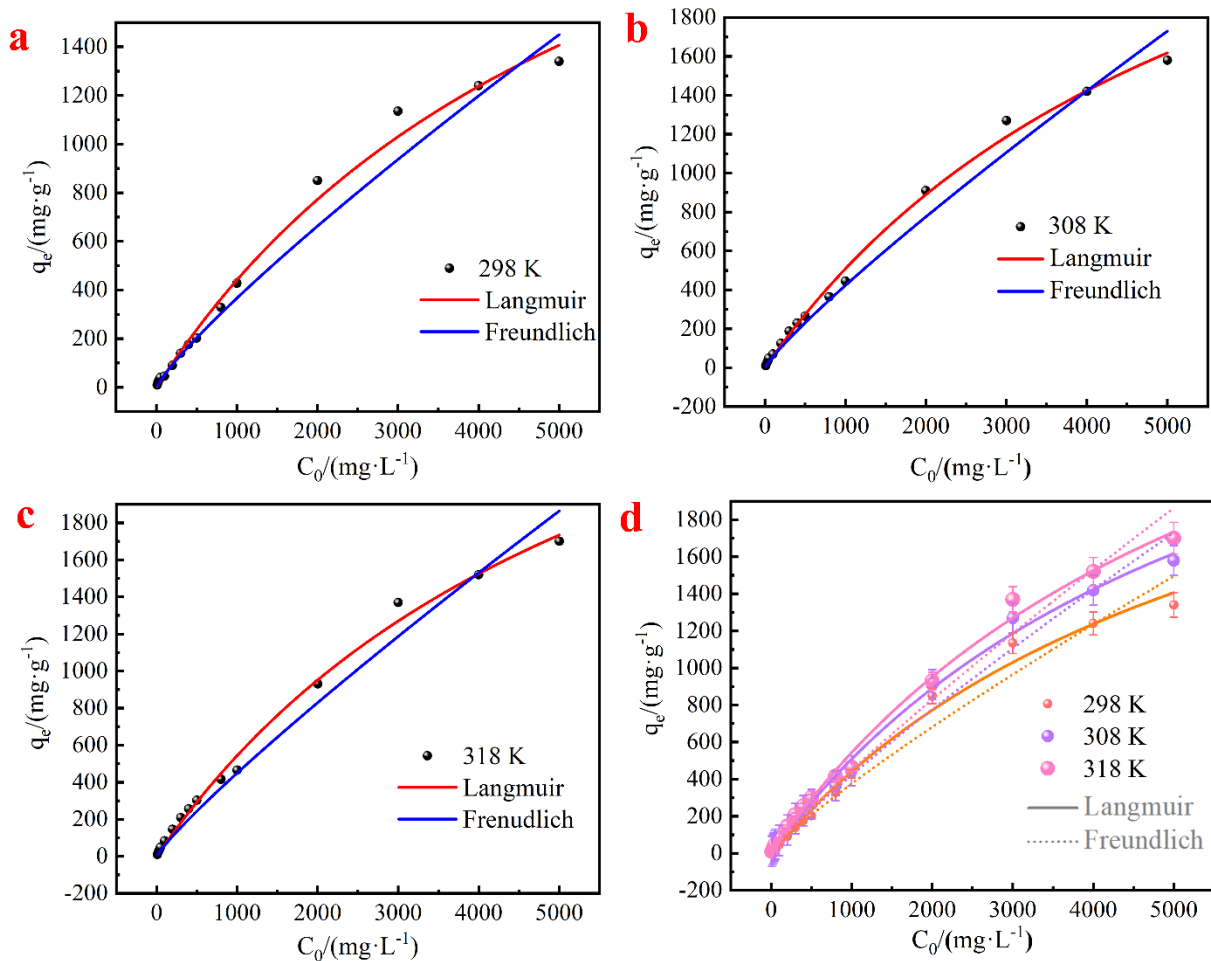
100
$$q_e = \frac{1}{n} \ln c_e + \ln K_F \quad (2)$$

101
$$R_L = \frac{1}{1 + K_L C_0} \quad (3)$$

102 where q_m ($\text{mg}\cdot\text{g}^{-1}$) is the theoretical maximum monolayer adsorption capacity, k_L is the Langmuir
103 constant ($\text{L}\cdot\text{g}^{-1}$), k_F is the Freundlich constant (mg/g) ($\text{L}\cdot\text{mg}^{-1}$)^{1/n}, $1/n$ represents the heterogeneity
104 factor, C_0 is the initial Cr(VI) concentration, and C_e is the Cr(VI) concentration at equilibrium.

105

106 **Figure S7**



107

108 **Fig. S7** The Langmuir model and Freundlich isotherm model fitting of Cr(VI) adsorption onto M-TT (pH = 4.4, T
109 = 298 K) (a), onto M-TT (pH = 4.4, T = 308 K) (b) and onto M-TT (pH = 4.4, T = 318 K) (c), and General
110 drawing (pH = 4.4, T = 298 K, T = 308 K, T = 318 K) (d).

111

112 **Table S2**

113 Two isotherm parameters for Cr(VI) adsorption onto M-TT (pH = 4.4, T = 298 K).

Samples	Langmuir Model			Freundlich Model		
	$q_{max} (mg \cdot g^{-1})$	$K_L (L/l)$	R^2	K_F	n	R^2
M-TT (298 K)	1655	0.00098	0.988	419.59	1.17	0.973
M-TT (308 K)	1666.67	0.00153	0.996	30.47	1.14	0.983
M-TT (318 K)	2000	0.00159	0.966	464	1.13	0.982

114

115 **Text S5**

116 The pseudo-first-order kinetic model, pseudo-second-order kinetic model, and intraparticle
 117 diffusion model are expressed as equations Eq. (4), Eq. (5), Eq. (6):

$$118 \quad \ln(q_e - q_t) = \ln q_e - k_1 t \quad (4)$$

$$119 \quad \frac{t}{q_t} = \frac{1}{k_2 q_e^2} + \frac{t}{q_e} \quad (5)$$

$$120 \quad q_t = k_{id} t^{1/2} + C \quad (6)$$

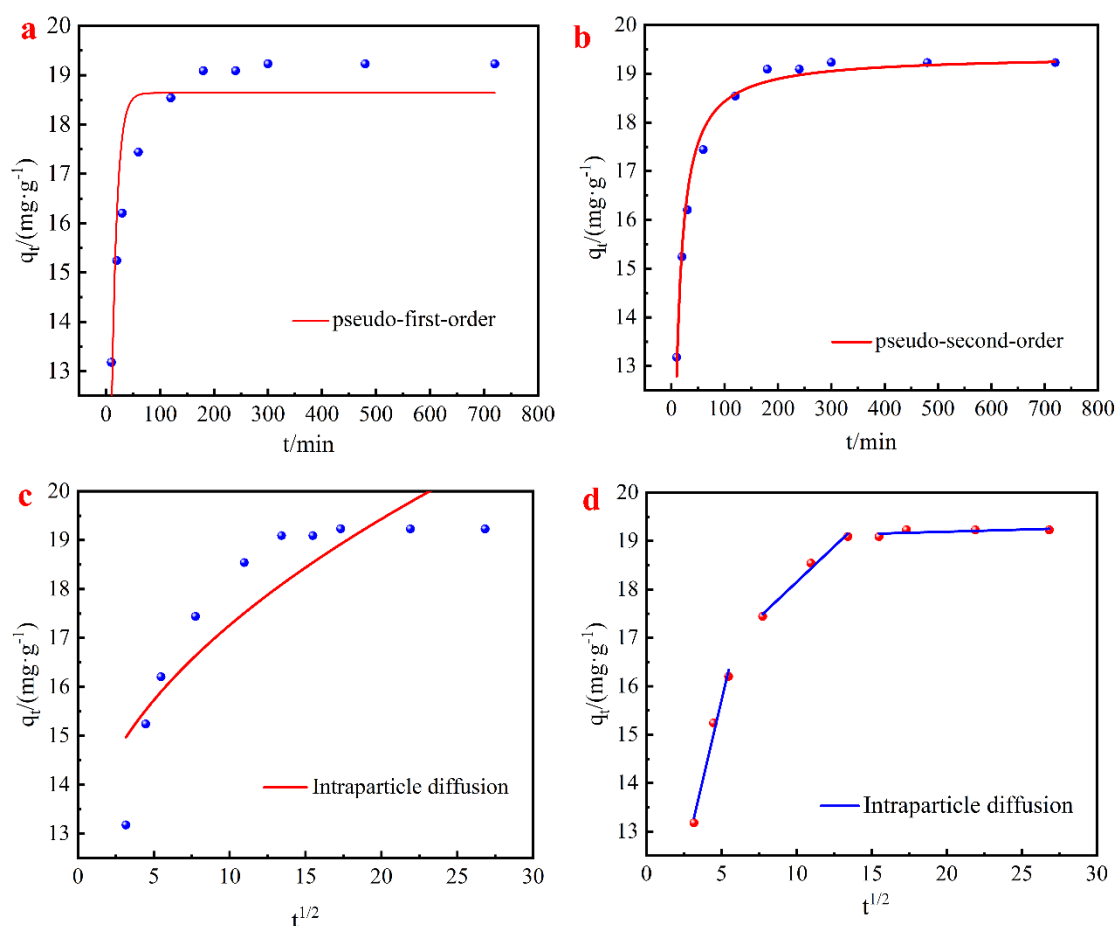
121 where q_e and q_t are the amounts of adsorbent Cr(VI) on the M-TT at equilibrium and at time t .

122 k_1 is the pseudo-first-order rate constant (min^{-1}). k_2 is the pseudo-second-order adsorption rate

123 constant. k_{id} is the intra-particle diffusion rate, and constant C is the intercept ($\text{mg} \cdot \text{g} \cdot \text{min}^{1/2}$).

124

125 **Figure S8**



126

127 **Fig. S8** The fitting of the pseudo-first-order kinetic model (a), the pseudo-second-order (b) and the intra-particle
 128 kinetic models (c, d) for Cr(VI) adsorption onto M-TT (pH = 4.4, T = 298 K, C₀ = 20 mg·L⁻¹).

129

130

131 **Table S3**

132 Kinetic parameters for Cr(VI) adsorption onto M-TT (pH = 4.4, T = 298 K, C₀ = 20 mg·L⁻¹).

Kinetic model	Parameter	Value	R ²
Pseudo-first-order	k_1 (min ⁻¹)	0.101	0.817
	q_e (mg·g ⁻¹)	18.64	
Pseudo-second-order	k_2 (mg·min ⁻¹ ·g ⁻¹)	0.0104	0.986
	q_e (mg·g ⁻¹)	19.406	
Intraparticle diffusion	k_{id} (mg·g ⁻¹)	1.656	0.785
	C (mg·g ⁻¹ ·min ⁻¹)	12.024	

133

134 **Text S6**

135 To investigate the effect of temperature on the adsorption capacity of Cr(VI), adsorption
 136 experiments were carried out at 298 K, 308 K and 318 K. The relevant thermodynamic parameters

137 are listed in Table S4, including Gibbs function change ΔG , enthalpy change ΔH , and entropy change
 138 ΔS , which are calculated from the following equations Eq. (7), Eq. (8), Eq. (9):

$$139 \quad \ln K_d = \frac{\Delta S}{R} - \frac{\Delta H}{T} \quad (7)$$

$$140 \quad \Delta G = \Delta H - T\Delta S = -RT\ln K_d \quad (8)$$

$$141 \quad K_d = \frac{c_0 - c_e}{c_e} \quad (9)$$

142 where K_d is the equilibrium constant ($\text{L}\cdot\text{g}^{-1}$), T is the temperature (K), and R is the standard gas
 143 constant ($8.314 \text{ J}\cdot\text{mol}^{-1}\cdot\text{K}^{-1}$).

144

145 **Table S4**

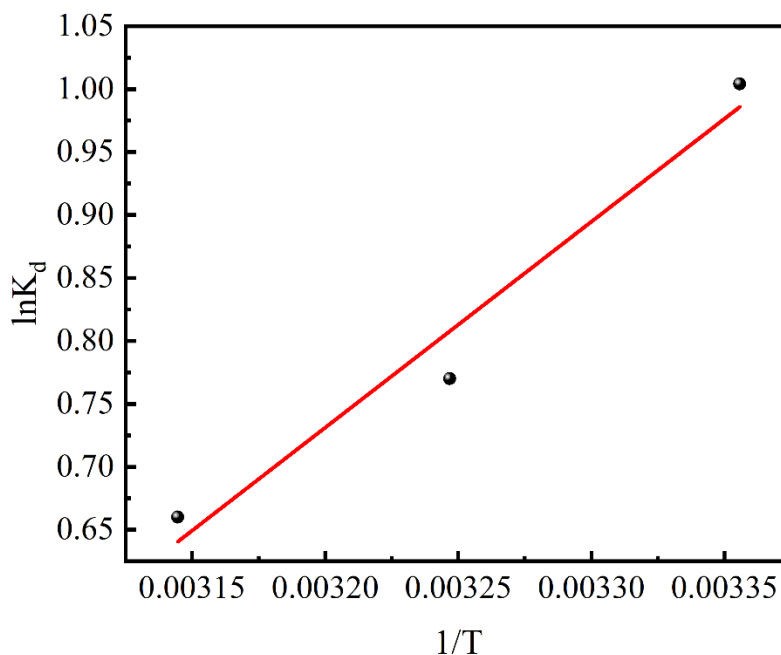
146 Thermodynamic parameters for Cr(VI) adsorption onto M-TT at different temperatures.

$K_d (\text{L}\cdot\text{g}^{-1})$			$\Delta G (\text{kJ mol}^{-1})$			ΔH	ΔS	R^2
298 K	308 K	318 K	298 K	308 K	318 K	($\text{kJ}\cdot\text{mol}^{-1}$)	($\text{J}\cdot\text{mol}^{-1}\cdot\text{K}^{-1}$)	
2.73	2.16	1.94	-2.49	-1.97	-1.75	334.25	1.13	0.97

147

148

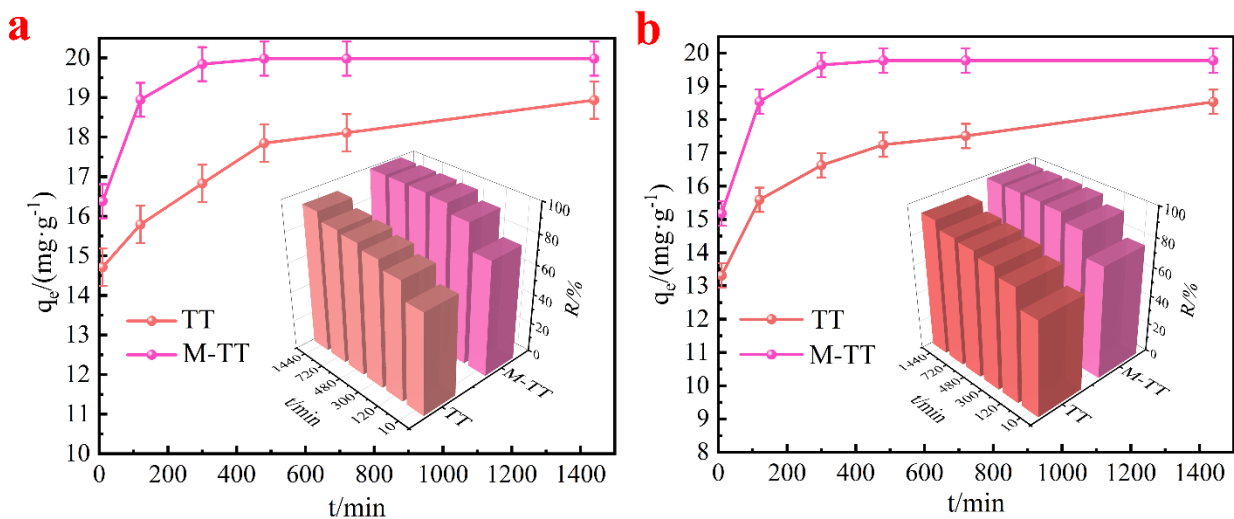
149 **Figure S9**



150

151

Fig. S9 Thermodynamic curve of Cr(VI) adsorption onto M-TT (pH = 4.4, T = 298 K, C₀ = 20 mg·L⁻¹).



153

154 **Fig. S10** Removal of Cr(VI) (a) and Cr(III) (b) by TT and M-TT (pH = 4.4, T = 298 K, C₀ = 20 mg·L⁻¹).

155 **Table S5**

156 The calculated adsorption energies of Cr atom on four sites of substrate material.

site	Adsorption energy (eV)
1	-0.193
2	-0.966
3	-1.080
4	-0.999

157

158

159

160

161

162

163

164

165

166

167

168

169

170

171

172

173

174

175

176 **Table S6**

177 Comparison before and after adsorption of other components in electroplating wastewater.

	Raw effluent	After treatment				
	Concentration	Raw effluent		Adjustive effluent		
	(mg/L)	Concentration	R%	Concentration	R%	
		(mg/L)		(mg/L)		
182	Cr(VI)	247.6	228.28	7.8	0.32	98.4
183	Cr(tot)	356.8	350.84	1.67	1.44	92.8
184	Li	1.17	0.998	15.15	0.026	3.76
	Ni	110.25	95.02	13.81	7.16	7.4
185	Zn	0.46	0.426	7.69	0.04	91.3
186	Pb	36.6	23.62	35.47	0.44	47.27
186	Co	17.05	9.597	43.72	0.118	69.58
187	pH	12.69	12.69		4.4	

188

189 *Adjust the concentration of Cr(VI) in the wastewater to 20 mg·L⁻¹, the pH value to 4.4, and the dosage to 1 g·L⁻¹.

190